Quantitative Structure–Activity Relationship (QSAR) Analysis of Tumor-specificity of 1,2,3,4-Tetrahydroisoquinoline Derivatives

YOSHIHIRO UESAWA[1], KIMINORI MOHRI[1], MASAMI KAWASE[2], MARIKO ISHIHARA[3] and HIROSHI SAKAGAMI[4]

[1]Clinical Pharmaceutics Laboratory, Meiji Pharmaceutical University, Noshio, Kiyose, Tokyo, Japan; [2]Faculty of Pharmaceutical Sciences, Matsuyama University, Matsuyama, Japan; Divisions of [3]Basic Chemistry and [4]Pharmacology, Meikai University School of Dentistry, Sakado, Saitama, Japan

Abstract. *Background: We have previously reported on the relative cytotoxicity of a total of 38 1,2,3,4-tetrahydroisoquinoline derivatives against human oral squamous cell carcinoma cell lines and human normal oral cells, and the correlation between the cytotoxicity and 17 chemical descriptors. However, the correlation between the tumor-specificity of these compounds and the chemical descriptors has never been investigated so far. Using these previous data, we investigated various parameters for their applicability in predicting tumor specificity. Materials and Methods: Original data of 50% cytotoxic concentration (CC_{50}) values exceeding the maximum concentration in experimental conditions were corrected by the introduction of a harmonic mean, reducing the number of compounds analyzed to 30. The mean pCC_{50} (=–log CC_{50}) values for normal and tumor cells were defined as N and T, respectively. Tumor specificity was defined as the ratio of the difference of these values to their sum: (T–N)/(T+N). The chemical descriptors were obtained by quantum chemical calculations using semi-empirical (AM1, PM3, and PM6) and density functional theory methods. The relationship between the chemical descriptors and tumor specificity was analyzed by linear regression and artificial neural networks. Results: Out of 17 chemical descriptors, water–accessible surface area showed the highest correlation coefficient with tumor specificity, regardless of the method of calculation. Furthermore, neural network analysis demonstrated the importance of quantum chemical calculations in predicting the specificity of tetrahydroisoquinoline derivatives. Conclusion: The present study suggests the applicability of quantum chemical descriptor in the estimation of tumor specificity of related compounds.*

Correspondence to: Yoshihiro Uesawa, Clinical Pharmaceutics Laboratory, Meiji Pharmaceutical University, Noshio, Kiyose, Tokyo 204-8588, Japan. Tel and Fax: +81 424958892, e-mail: uesawa@my-pharm.ac.jp

Key Words: 1,2,3,4-Tetrahydroisoquinolins, QSAR, tumor-specificity index, semi-empirical molecular-orbital method, artificial neural network.

The incorporation of the 1-methyl-1,2,3,4-tetrahydroisoquinoline (TIQ) moiety is an important synthetic strategy in drug discovery (1), and in fact, TIQ is the only endogenous Parkinson-preventing agent discovered to date (2). The high therapeutic properties of the related drugs have encouraged medicinal chemists to synthesize a large number of novel chemotherapeutic agents. Pharmaceutical properties include antineoplastic (3, 4), nitric oxide (NO) inhibition (5), histamine H_3 antagonism and serotonin reuptake inhibition (6), α-amino-3-hydroxy-5-methyl-4-isoxazole propionic acid (AMPA) receptor antagonism (7), bradycardic (8), orexin-2 receptor–selective antagonism (9), multidrug–resistance (MDR) reversion (10-12), γ-secretase inhibition (13), kinase insert domain containing receptor (KDR) inhibition (14), and antidiabetic activities (15). All are unique characteristics of newly synthesized TIQ derivatives. The TIQ family of alkaloids also includes potent cytotoxic agents that display a range of biological properties, such as antitumor and antimicrobial activities (16).

TIQ derivatives were shown to induce neurotoxicity in various animals *via* the decline of ATP levels due to mitochondrial inhibition of complex 1, and DNA damage (2), and inactivation of Cu,Zn-superoxide dismutase, induced by free radical formation (17). TIQ derivatives possessing bulky alkyl group substituents such as 1-cyclobutyl-, 1-cyclohexyl-, 1-phenyl-, or 1-benzyl-, at the C-1 position showed significant cytotoxicity against rat PC12 cells (18). This was confirmed by our recent finding that among 38 newly synthesized TIQ derivatives, TD1-to-19 (Figure 1A) and TQ1-to-19 (Figure 1B), (6,7-dimethoxy-3,4-dihydroisoquinolin-2(1*H*)-yl)(3,4-dimethoxyphenyl)methanone (TQ9), with has bulky

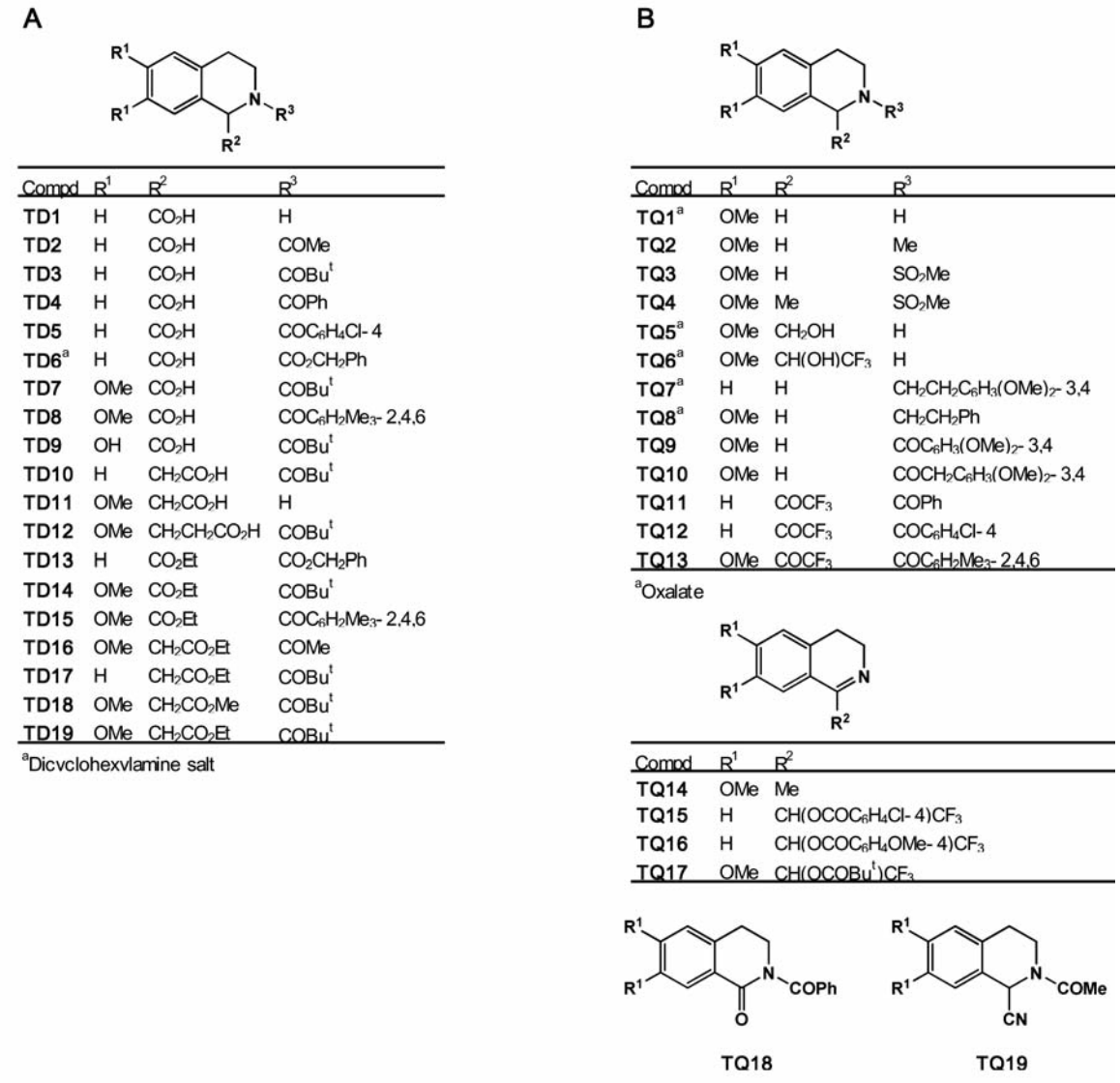

Compd	R^1	R^2	R^3
TD1	H	CO_2H	H
TD2	H	CO_2H	COMe
TD3	H	CO_2H	$COBu^t$
TD4	H	CO_2H	COPh
TD5	H	CO_2H	COC_6H_4Cl-4
TD6[a]	H	CO_2H	CO_2CH_2Ph
TD7	OMe	CO_2H	$COBu^t$
TD8	OMe	CO_2H	$COC_6H_2Me_3$-2,4,6
TD9	OH	CO_2H	$COBu^t$
TD10	H	CH_2CO_2H	$COBu^t$
TD11	OMe	CH_2CO_2H	H
TD12	OMe	$CH_2CH_2CO_2H$	$COBu^t$
TD13	H	CO_2Et	CO_2CH_2Ph
TD14	OMe	CO_2Et	$COBu^t$
TD15	OMe	CO_2Et	$COC_6H_2Me_3$-2,4,6
TD16	OMe	CH_2CO_2Et	COMe
TD17	H	CH_2CO_2Et	$COBu^t$
TD18	OMe	CH_2CO_2Me	$COBu^t$
TD19	OMe	CH_2CO_2Et	$COBu^t$

[a]Dicyclohexylamine salt

Compd	R^1	R^2	R^3
TQ1[a]	OMe	H	H
TQ2	OMe	H	Me
TQ3	OMe	H	SO_2Me
TQ4	OMe	Me	SO_2Me
TQ5[a]	OMe	CH_2OH	H
TQ6[a]	OMe	$CH(OH)CF_3$	H
TQ7[a]	H	H	$CH_2CH_2C_6H_3(OMe)_2$-3,4
TQ8[a]	OMe	H	CH_2CH_2Ph
TQ9	OMe	H	$COC_6H_3(OMe)_2$-3,4
TQ10	OMe	H	$COCH_2C_6H_3(OMe)_2$-3,4
TQ11	H	$COCF_3$	COPh
TQ12	H	$COCF_3$	COC_6H_4Cl-4
TQ13	OMe	$COCF_3$	$COC_6H_2Me_3$-2,4,6

[a]Oxalate

Compd	R^1	R^2
TQ14	OMe	Me
TQ15	H	$CH(OCOC_6H_4Cl$-4$)CF_3$
TQ16	H	$CH(OCOC_6H_4OMe$-4$)CF_3$
TQ17	OMe	$CH(OCOBu^t)CF_3$

Figure 1. *Structures of the 1,2,3,4-tetrahydroisoquinoline derivatives.*

substituents (such as a 3,4-dimethoxybenzoyl group), and ethyl 2-benzyloxycarbonyl-1,2,3,4-tetrahydroisoquinoline-1-carboxylate (TD13), which has an ethoxycarbonyl group and a benzyloxycarbonyl group, showed the highest tumor specific cytotoxicity (TS=12.5 and 5.3, respectively) towards human oral squamous cell carcinoma (OSCC) (19).

We previously applied a quantitative structure–activity relationship (QASR) analysis to delineate the relationship between the cytotoxicity (evaluated by 50% cytotoxic concentration, CC_{50}) of these TIQ derivatives, their molecular weight and 17 chemical parameters (descriptors), using a semi-empirical molecular-orbital method (CAChe 4.9, PM5). There was a good correlation between the CC_{50} of TQ1-to-19 and their hydrophobicity (*log*P) and the descriptors for the molecular size such as surface area, volume and width (20). The cytotoxicity of TD1-to-19 depended on hydrophobicity and the distance between C–R2 in the 3-dimensional configuration (21).

However, the relationship between tumor specificity and these chemical descriptors has not yet been reported. We therefore investigated the correlation between tumor specificity of TIQ derivatives and various chemical descriptors.

Materials and Methods

Preparation of 1,2,3,4-tetrahydroisoquinoline (TIQ) derivatives. Thirty–eight TIQ derivatives (Figure 1) were prepared as described elsewhere (19).

Table I. *Estimated 50% cytotoxic concentration (CC_{50}), average log CC_{50}^{-1} (pCC_{50}), and tumor-specificity index values of 38 1,2,3,4-tetrahydroisoquinoline derivatives. N1, N2, and N3 represent human normal cells, gingival fibroblast HGF, pulp cell HPC, and periodontal ligament fibroblast HPLF, respectively. T1, T2, T3, and T4 represent human OSCC cell lines (HSC-2, HSC-3, HSC-4) and human promyelocytic leukemic HL-60 cells, respectively.*

Comp. no.	Estimated CC_{50} (mM)							Average pCC_{50}		Tumor-specificity index
	N1	N2	N3	T1	T2	T3	T4	N	T	(T–N)/(T+N)
TD1	0.800	0.800	0.800	0.800	0.800	0.800	0.800	0.097	0.097	0.000
TD2	0.800	0.800	0.800	0.800	0.800	0.800	0.800	0.097	0.097	0.000
TD3	0.800	0.800	0.800	0.800	0.800	0.800	0.800	0.097	0.097	0.000
TD4	0.800	0.800	0.800	0.800	0.800	0.800	0.788	0.097	0.099	0.008
TD5	0.800	0.800	0.800	0.800	0.800	0.800	0.342	0.097	0.189	0.323
TD6	0.800	0.800	0.800	0.800	0.800	0.800	0.199	0.097	0.248	0.438
TD7	0.800	0.800	0.800	0.800	0.800	0.800	0.800	0.097	0.097	0.000
TD8	0.309	0.330	0.690	0.730	0.800	0.772	0.131	0.384	0.307	–0.111
TD9	0.800	0.800	0.800	0.728	0.752	0.784	0.146	0.097	0.301	0.513
TD10	0.800	0.800	0.800	0.800	0.800	0.800	0.720	0.097	0.108	0.056
TD11	0.800	0.800	0.800	0.115	0.275	0.072	0.108	0.097	0.902	0.806
TD12	0.800	0.800	0.800	0.800	0.800	0.800	0.792	0.097	0.098	0.006
TD13	0.301	0.272	0.226	0.061	0.063	0.072	0.010	0.578	1.389	0.413
TD14	0.748	0.764	0.792	0.708	0.800	0.800	0.088	0.115	0.350	0.506
TD15	0.120	0.134	0.108	0.068	0.064	0.083	0.016	0.920	1.310	0.175
TD16	0.800	0.800	0.800	0.800	0.800	0.800	0.201	0.097	0.247	0.436
TD17	0.325	0.344	0.324	0.258	0.307	0.300	0.038	0.480	0.761	0.226
TD18	0.336	0.714	0.710	0.706	0.800	0.780	0.112	0.256	0.327	0.121
TD19	0.314	0.317	0.315	0.706	0.782	0.746	0.084	0.501	0.365	–0.157
TQ1	0.728	0.764	0.742	0.167	0.310	0.343	0.315	0.128	0.563	0.629
TQ2	0.772	0.800	0.774	0.800	0.800	0.756	0.790	0.107	0.104	–0.012
TQ3	0.800	0.800	0.800	0.710	0.800	0.800	0.336	0.097	0.204	0.356
TQ4	0.720	0.780	0.794	0.790	0.800	0.800	0.293	0.117	0.207	0.279
TQ5	0.708	0.800	0.748	0.176	0.248	0.175	0.193	0.124	0.708	0.701
TQ6	0.800	0.800	0.800	0.740	0.800	0.800	0.326	0.097	0.203	0.353
TQ7	0.307	0.313	0.299	0.276	0.298	0.250	0.071	0.514	0.709	0.160
TQ8	0.298	0.318	0.289	0.255	0.238	0.222	0.087	0.521	0.733	0.169
TQ9	0.334	0.346	0.282	0.020	0.042	0.030	0.010	0.496	1.650	0.538
TQ10	0.279	0.314	0.303	0.296	0.794	0.358	0.098	0.525	0.521	–0.004
TQ11	0.272	0.282	0.249	0.116	0.083	0.092	0.032	0.573	1.137	0.330
TQ12	0.348	0.742	0.650	0.161	0.166	0.148	0.038	0.258	0.956	0.574
TQ13	0.274	0.232	0.172	0.131	0.097	0.115	0.027	0.654	1.101	0.255
TQ14	0.800	0.800	0.768	0.329	0.363	0.282	0.746	0.103	0.400	0.591
TQ15	0.287	0.256	0.291	0.209	0.155	0.153	0.043	0.557	0.918	0.245
TQ16	0.264	0.209	0.184	0.105	0.080	0.080	0.032	0.664	1.167	0.274
TQ17	0.269	0.261	0.226	0.152	0.141	0.182	0.030	0.600	0.983	0.242
TQ18	0.287	0.306	0.273	0.266	0.240	0.248	0.085	0.540	0.718	0.141
TQ19	0.728	0.800	0.754	0.778	0.800	0.800	0.255	0.119	0.224	0.306

N1, N2, and N3 mean human normal cells, gingival fibroblast HGF, pulp cell HPC, and periodontal ligament fibroblast HPLF, respectively. T1, T2, T3, and T4 mean human OSCC cell lines (HSC-2, HSC-3, HSC-4) and human promyelocytic leukemic HL-60 cells, respectively.

Determination of CC_{50}. Three human OSCC cell lines (HSC-2, HSC-3, HSC-4) (purchased from Riken Cell Bank, Tsukuba, Japan), three human normal cells (gingival fibroblast HGF, pulp cell HPC, periodontal ligament fibroblast HPLF) (established as described previously (19)), and human promyelocytic leukemic HL-60 cells (purchased from Riken Cell Bank) were treated for 48 h with different concentrations of test compounds. The 50% cytotoxic concentration (CC_{50}) was determined from the dose–response curve (19). The original data of CC_{50} values (mM) are listed in Table I where names of tumor cells (HSC-2, HSC-3, HSC-4, and HL-60) are indicated by T1, T2, T3, and T4, respectively, and normal cells (HGF, HPC, and HPLF) by N1, N2, and N3, respectively.

Estimation of CC_{50} values. Original data contain the sign of inequality such as '>'. For the convenience of analysis, these values were changed into forms suitable for the arithmetic calculation. Since '>400' is equal to '400~∞', we calculated the harmonic mean as follows: 1/(average(1/400,1/∞))=800

As a result of the estimation by harmonic mean, the value became two-fold (Table I). Eight compounds, TD1, TD2, TD3, TD4,

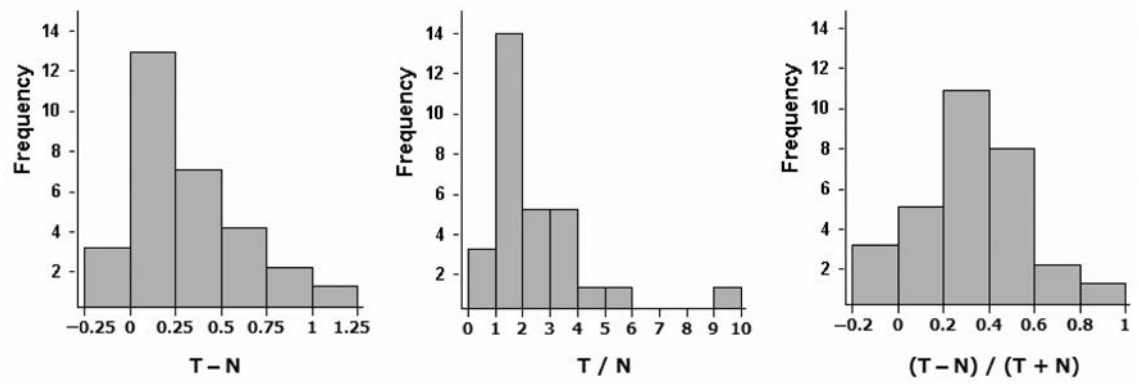

Figure 2. *Comparison of normality produced by three calculation approaches: T–N, T/N, and (T–N)/(T+N), where N and T are the estimated 50% cytotoxic concentrations of agent against normal and tumor cells, respectively.*

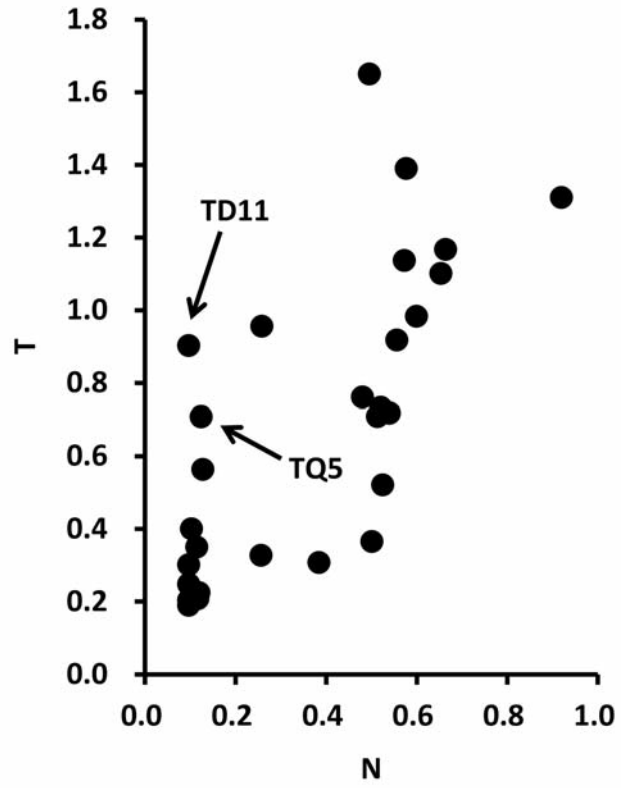

Figure 3. *Correlation between N and T, where N and T are the estimated 50% cytotoxic concentrations of agent against normal and tumor cells, respectively.*

TD7, TD10, TD12, and TQ2, which had estimated CC_{50} values >400 μM for all 7 cell lines were omitted, since the validity of their tumor specificity value calculated is very low. Therefore, the number of compounds analyzed was reduced from 38 to 30.

Inverse logarithmic ratio. In the case of inhibition constant (Ki), which shows a logarithmic normal distribution, the use of pKi (=–*log* Ki) instead of Ki facilitates the analysis. Since the CC_{50} values had a distribution pattern close to the logarithmic normal distribution, we used the pCC_{50} (=–log CC_{50}) (Table I).

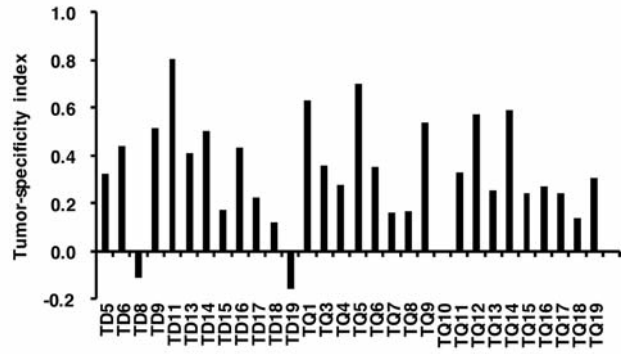

Figure 4. *The tumor-specificity index for each compound as given by (T-N)/(T+N), where N and T are the estimated 50% cytotoxic concentrations of agent against normal and tumor cells, respectively.*

Mean values. The mean pCC_{50} values for normal cells and tumor cell lines were defined as N and T, respectively (Table I).

Calculation of the representative value for tumor specificity. Parameters that indicate tumor specificity were determined for each compound. It is conceivable that this parameter is defined by the balance between pCC_{50} values for normal cells and that for tumor cell lines (N, T). The following three parameters are available: (i) difference (T–N), (ii) ratio (T/N) and (iii) ratio of difference to their sum: (T–N)/(T+N). Of these, (T–N)/(T+N) produced the highest normality (Figure 2) and correlation coefficient with chemical descriptors (data not shown). Furthermore, the ratio of T/N produced the same value, whenever both T and N had higher or low values. On the other hand, the ratio of (T–N)/(T+N) produced a higher correlation coefficient for compounds with lower cytotoxicity. Based on these considerations, (T–N)/(T+N) was used for the following analyses as a tumor-specificity index.

Calculation of chemical descriptors. Spartan10 for Windows (Wavefunction, Inc., Irvine, CA, USA) was used for the calculations.

Table II. *Quantum chemical parameters calculated by PM3*.

Comp. no.	Energy (au)	E_{HOMO} (au)	E_{LUMO} (au)	Dipole moment (debye)	MSA	MV (Å^2)	PSA (Å^3)	WSA (Å^2)	χ (Å^2)	η (au)	ω (au)	EPmin (au)	EPmax (au)	Ovality (au)	Log P	HBD	HBA
TD5	–0.130	–0.356	–0.0170	4.33	314.1	300.3	49.1	168.5	0.186	0.169	0.103	–0.105	0.0485	1.448	0.498	1	3
TD6	–0.128	–0.353	–0.0005	4.69	316.4	305.2	48.7	173.3	0.177	0.176	0.089	–0.108	0.0469	1.443	0.578	1	3
TD8	–0.276	–0.334	–0.0054	3.53	415.7	395.4	62.8	219.8	0.170	0.164	0.088	–0.110	0.0483	1.596	–0.791	1	5
TD9	–0.337	–0.330	–0.0005	2.93	303.9	288.9	85.8	156.9	0.165	0.165	0.083	–0.107	0.0528	1.438	–0.704	3	5
TD11	–0.232	–0.343	–0.0009	2.59	278.5	254.7	61.6	150.1	0.172	0.171	0.086	–0.100	0.0471	1.433	–1.946	1	4
TD13	–0.125	–0.350	0.0000	4.62	354.8	343.9	34.6	189.2	0.175	0.175	0.088	–0.107	0.0344	1.495	1.179	0	3
TD14	–0.305	–0.332	–0.0021	3.45	390.0	368.5	46.8	209.0	0.167	0.165	0.084	–0.108	0.0296	1.569	0.112	0	5
TD15	–0.272	–0.346	–0.0072	2.26	460.5	435.0	49.7	245.1	0.177	0.170	0.092	–0.112	0.0235	1.658	–0.189	0	5
TD16	–0.296	–0.348	–0.0063	2.85	362.2	334.3	50.6	197.4	0.177	0.171	0.092	–0.109	0.0363	1.555	–1.697	0	5
TD17	–0.201	–0.351	0.0048	2.17	347.0	332.0	35.0	192.1	0.173	0.178	0.084	–0.105	0.0327	1.497	2.182	0	3
TD18	–0.307	–0.329	0.0024	2.92	389.0	368.3	48.7	213.0	0.163	0.166	0.081	–0.107	0.0326	1.565	–0.108	0	5
TD19	–0.315	–0.329	0.0027	2.88	409.5	386.8	48.5	224.2	0.163	0.166	0.080	–0.109	0.0323	1.595	0.230	0	5
TQ1	–0.086	–0.335	0.0036	1.50	230.8	208.7	27.3	141.6	0.166	0.169	0.081	–0.098	0.0336	1.356	–1.485	0	3
TQ3	–0.196	–0.343	–0.0166	4.60	291.9	263.0	51.0	158.7	0.180	0.163	0.099	–0.140	0.0731	1.471	–2.001	0	6
TQ4	–0.206	–0.352	–0.0148	4.48	310.1	281.3	50.8	165.4	0.183	0.169	0.100	–0.140	0.0695	1.494	–1.683	0	6
TQ5	–0.157	–0.337	0.0018	2.28	257.7	234.3	46.8	146.8	0.168	0.169	0.083	–0.094	0.0530	1.402	–2.022	1	4
TQ6	–0.406	–0.353	–0.0122	2.43	290.4	266.8	44.9	138.0	0.183	0.170	0.098	–0.080	0.0473	1.449	–1.063	1	4
TQ7	–0.054	–0.334	0.0015	0.86	352.2	330.6	17.1	213.3	0.166	0.168	0.082	–0.100	0.0201	1.523	0.106	0	3
TQ8	–0.054	–0.333	0.0036	1.39	352.5	330.6	17.1	210.4	0.165	0.169	0.081	–0.096	0.0209	1.524	0.106	0	3
TQ9	–0.216	–0.339	–0.0089	2.70	394.5	369.3	44.9	222.9	0.174	0.165	0.092	–0.109	0.0332	1.585	–2.690	0	6
TQ10	–0.227	–0.347	–0.0055	1.75	413.8	387.8	45.9	209.6	0.176	0.171	0.091	–0.105	0.0354	1.609	–2.746	0	6
TQ11	–0.274	–0.356	–0.0162	5.48	327.1	313.3	29.7	161.8	0.186	0.170	0.102	–0.105	0.0351	1.466	2.286	0	3
TQ12	–0.284	–0.358	–0.0203	5.05	341.9	326.4	29.7	163.4	0.189	0.169	0.106	–0.104	0.0363	1.491	2.151	0	3
TQ13	–0.429	–0.354	–0.0212	5.45	444.7	421.8	44.0	212.9	0.187	0.166	0.106	–0.108	0.0376	1.635	0.862	0	5
TQ14	–0.072	–0.340	–0.0184	1.52	243.4	221.9	21.7	153.7	0.179	0.161	0.100	–0.109	0.0235	1.373	–0.527	0	3
TQ15	–0.280	–0.352	–0.0303	3.20	349.0	327.2	26.1	192.4	0.191	0.161	0.114	–0.104	0.0336	1.520	3.050	0	2
TQ16	–0.332	–0.350	–0.0217	2.99	364.0	341.3	33.1	205.4	0.186	0.164	0.105	–0.105	0.0325	1.541	2.210	0	3
TQ17	–0.463	–0.347	–0.0277	2.53	391.2	357.7	41.1	196.2	0.187	0.160	0.110	–0.101	0.0365	1.605	2.062	0	4
TQ18	–0.038	–0.362	–0.0210	3.33	275.0	262.6	28.9	170.4	0.191	0.170	0.107	–0.104	0.0291	1.387	1.091	0	3
TQ19	0.055	–0.326	–0.0239	4.53	224.5	209.5	30.2	142.3	0.175	0.151	0.101	–0.109	0.0436	1.316	0.314	0	3

E_{HOMO}: Highest occupied molecular orbital energy; E_{LUMO}: lowest unoccupied molecular orbital energy; MSA: surface area of the molecule; MV: volume of the molecule; PSA: polar surface area; WSA: water–accessible surface area; χ: negativity; η: absolute hardness; ω: reactivity index; EPmin: minimal electrostatic potential; EPmax: maximal electrostatic potential; HBA: hydrogen-bond acceptor; HBD: hydrogen-bond donor.

Each structure was optimized with Merck Molecular Force Field (MMFFaq), and then checked by the semi-empirical method (AM1, PM3, PM6) and density functional theory (DFT-B3LYP/6-31+G*). During each step of the calculation, quantum chemical, molecular shape, and molecular property parameters were obtained. The parameters used were: energy (au), highest occupied molecular orbital (HOMO) energy (E_{HOMO}; au), lowest unoccupied molecular orbital (LUMO) energy (E_{LUMO}; au), dipole moment (debye), surface area of the molecule (MSA; Å^2), volume of the molecule (MV; Å^3), polar surface area (PSA; Å^2), hydrogen-bond acceptor (HBA), hydrogen-bond donor (HBD), negativity [$\chi=-(E_{LUMO}+E_{HOMO})/2$], absolute hardness [$\eta=(E_{UMO}-E_{HOMO})/2$], reactivity index ($\omega=\chi^2/2\eta$), ovality, hydrophobicity (*log*P), minimal and maximal electrostatic potentials (EPmin and EPmax; au), and water–accessible surface area (WSA; Å^2). These had different values in each calculation method used for precise structural determination.

Statistical analysis. We determined the relationship between N and T (Figure 3) and the tumor-specificity index (T–N)/(T+N) for each chemical descriptor (Figure 4). We attempted to construct a tumor-specificity estimation model using artificial neural networks. Thirty compounds were divided at random into two sets, one consisting of 24 compounds (training set for construction of the model: TD6, TD8, TD9, TD11, TD13, TD15, TD16, TD17, TD18, TD19, TQ1, TQ3, TQ6, TQ8, TQ9, TQ10, TQ11, TQ12, TQ14, TQ15, TQ16, TQ17, TQ18, and TQ19) and the other consisting of 6 compounds (test set for confirmation of the model: TD5, TD14, TQ4, TQ5, TQ7, and TQ13). Using major PM3 descriptors and the 'neuralnet' script in JMP ver.9 (SAS Institute Inc., Cary, NC, U.S.A.) for calculation, an estimation model was constructed from a nonlinear regression of multilayer perception neural networks employing back propagation-training algorithm. Descriptor selection was performed with the leave-one-out cross validation. The model constructed was validated by prediction of the test set compounds.

Results and Discussion

Correlation between N and T. The structures of TD11 and TQ5 are desirable for chemotherapy (Figure 3) because of

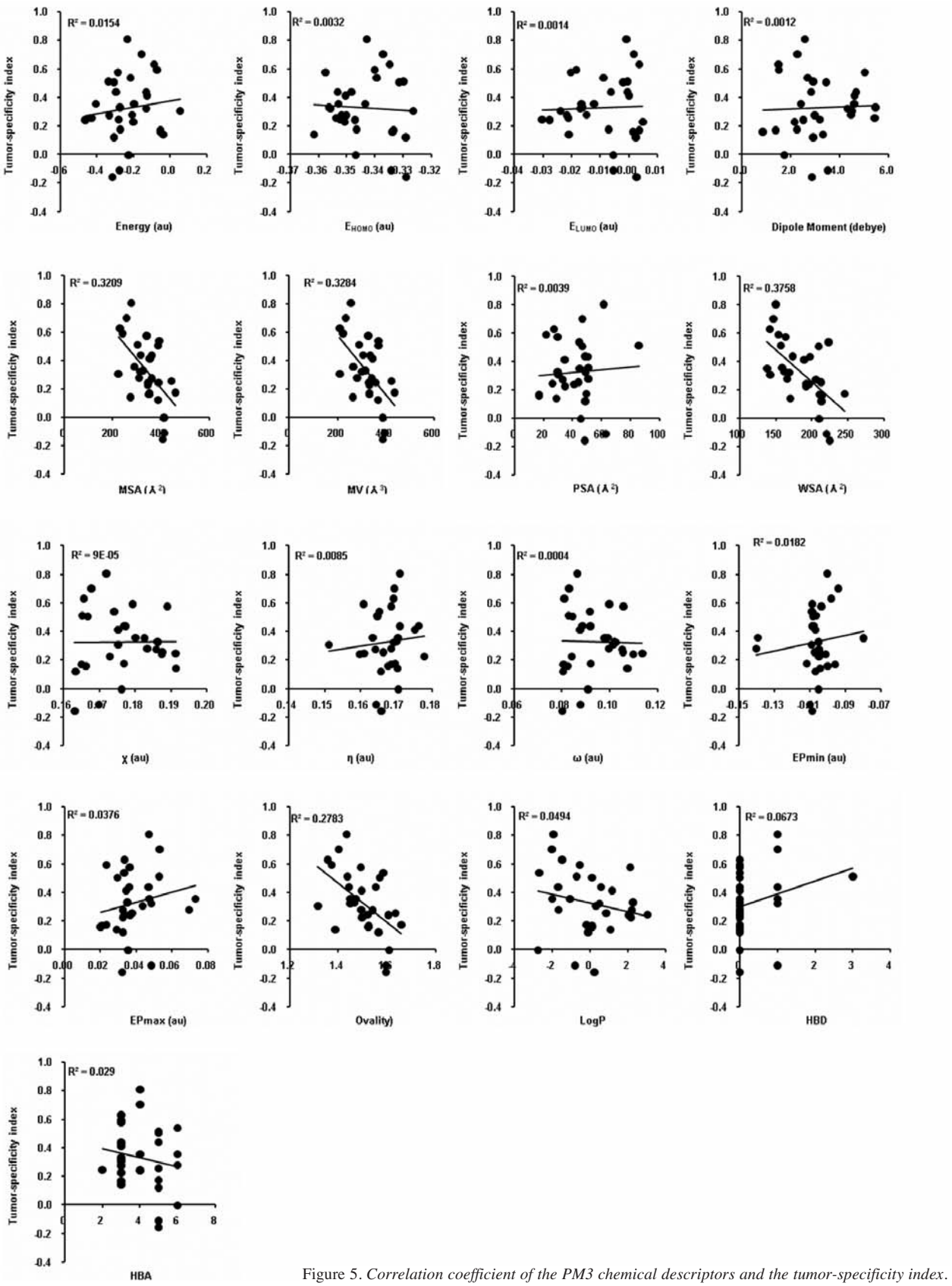

Figure 5. *Correlation coefficient of the PM3 chemical descriptors and the tumor-specificity index.*

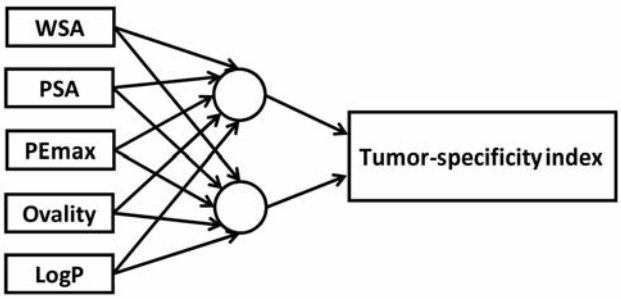

Figure 6. *Input, hidden, and output layers in the artificial neural network model.*

high T and the low N values. The tumor-specificity index of each compound is shown in Figure 4. Both TD11 and TQ5 had high values of a tentative cut-off point of 0.7 units. Both compounds include methoxy groups and hydrogen at R^1 and R^3 positions, respectively, of the tetrahydroisoquinoline skeleton (Figure 1). These structural properties may be responsible for the tumor-specificity.

Correlation between each chemical descriptor and tumor-specificity index. Regardless of the calculation method used, the best correlation was shown between WSA and tumor-specificity index. That is, the determined coefficients (r^2) for the index and WSA calculated by AM1, PM3, PM6, and DFT-B3LYP/6-31+G* methods were 0.357, 0.376, 0.338, and 0.374, respectively, suggesting that WSA calculated by PM3, as well as DFT, is a useful chemical descriptor to evaluate the tumor-specificity. Scatter plots with correlation coefficients obtained in the linear regression analyses on PM3 chemical descriptors (Table II) and tumor-specificity index are shown in Figure 5.

Artificial neural network. Neural networks are powerful tools for the numerical formulation of nonlinear relationships, although it is difficult to determine how much each descriptor contributes to the constructed model. As a result of trials for variable selection, we constructed a model with 5 descriptors in an input layer (WSA, PSA, PEmax, ovality and logP) and 2 nodes in a hidden layer (Figure 6). Training and test sets enabled the successful construction of a model that can predict tumor specificity at a high probability ($R^2_{training}$=0.909, $Q^2_{leave\text{-}one\text{-}out}$=0.543, R^2_{test}=0.923). This suggests that these quantum chemical descriptors have the most information on tumor specificity and can be used to estimate the tumor specificity of related compounds (Figure 7).

Conclusion

The present study demonstrates for the first time that there is a significant correlation between the tumor-specificity of TIQ derivatives and WSA. Furthermore, we succeeded in constructing a predictive neural network model for tumor specificity with 5 parameters, including WSA and logP.

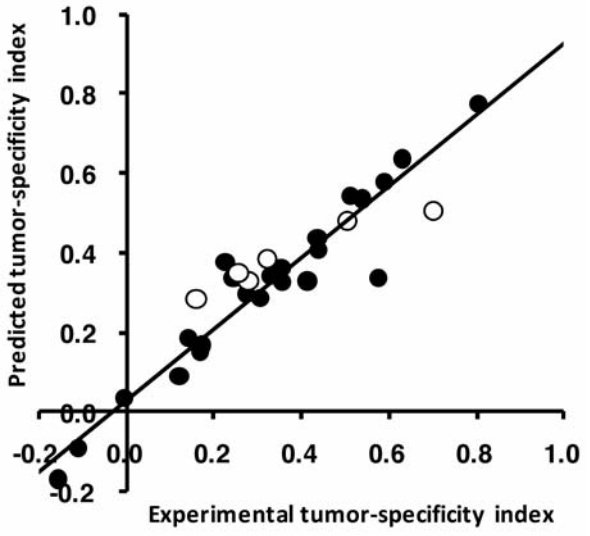

Figure 7. *Scatter plots between the experimental tumor-specificity indices and those predicted by the artificial neural network model using the descriptors shown in Figure 6. Training set and test set compounds are indicated by closed and open symbols, respectively.*

References

1 Page D, Nguyen N, Bernard S, Coupal M, Gosselin M, Lepage J, Adam L and Brown W: New scaffolds in the development of mu opioid-receptor ligands. Bioorg Med Chem Lett *13*: 1585-1589, 2003.

2 Abe K, Saitoh T, Horiguchi Y, Utsunomiya I and Taguchi K: Review. Synthesis and neurotoxicity of tetrahydroisoquinoline derivatives for studying Parkinson's disease. Biol Pharm Bull *28*: 1355-1362, 2005.

3 Mohler ML, Kang G-S, Hong S-S, Patil R, Kirichenko OV, Li W, Rakov IM, Geisert EE and Miller DD: Discovery of antiglioma activity of biaryl 1,2,3,4-tetrahydroisoquinoline derivatives and conformationally flexible analogues. J Med Chem *49*: 5845-5848, 2006.

4 Lin H-R, Safo MK and Abraham DJ: Identification of a series of teterhydroisoquinoline derivatives as potential therapeutic agents for breast cancer. Bioorg Med Chem Lett *17*: 2581-2589, 2007.

5 Seo JW, Srisook E, Son HJ, Hwang O, Cha Y-N and Chi DY: Syntheses of terahydroisoquinoline derivatives that inhibit NO production in activated BV-2 microglial cells. Eur J Med Chem *43*: 1160-1170, 2008.

6 Letavic MA, Keith JM, Jablonowski JA, Stocking EM, Gomez LA, Ly KS, Miller JM, Barbier AJ, Bonaventure P, Boggs JD, Wilson SJ, Miller KL, Lord B, McAllister HM, Tognarelli DJ, Wu J, Abad MC, Schubert C, Lovenberg TW and Carruther NI: Novel tetrahydroisoquinolines are histamine H3 antagonists and serotonin reuptake inhibitors. Bioorg Med Chem Lett *17*: 1047-1051, 2007.

7 Gitto R, Ficarra R, Stancanelli R, Guardo M, De Luca L, Barreca ML, Pagano B, Rotondo A, Bruno G, Russo E, De Sarro G and Chimirri A: Synthesis, resolution, stereochemistry, and molecular modeling of (*R*)- and (*S*)-2-acetyl-1-(4'-chlorophenyl)-6,7-dimethoxy-1,2,3,4-tetrahydroisoquinoline AMPAR antagonists. Bioorg Med Chem *15*: 5417-5423, 2007.

8 Kubota H, Watanabe T, Kakefuda A, Masuda N, Wada K, Ishii N, Sakamoto S and Tsukamoto S: Synthesis and pharmacological evaluation of piperidinoalkanoyl-1,2,3,4-tetrahydroisoquinoline derivatives as novel specific bradycardic agents. Bioorg Med Chem Lett *14*: 3049-3052, 2004.

9 Hirose M, Egashira S, Goto Y, Hashihayata T, Ohtake N, Iwaasa H, Hata M, Fukami T, Kanatani A and Yamada K: N-Acyl 6,7-dimethoxy-1,2,3,4-tetrahydroisoquinoline: the first orexin-2 receptor selective non-peptidic antagonist. Bioorg Med Chem Lett *13*: 4497-4499, 2003.

10 Fang W, Li Y, Cai Y, Kang K, Yan F, Liu G and Huang W: Substituted tetrahydroisoquinoline compounds B3 inhibited P-glycoprotein-mediated multidrug resitance *in vitro* and *in vivo*. J Pharm Pharmacol *59*: 1649-1655, 2007.

11 Yan F, Jiang Y, Li Y-M, Zhen X, Cen J and Fang W-R: Reversal of P-glycoprotein and multidrug resistance-associated protein 1-mediated multidrug resistance in cancer cells by HZ08 isomers, tetraisohydroquinoline derivatives. Biol Pharm Bull *31*: 1258-1264, 2008.

12 Li Y, Zhang H-B, Huang W-L and Li Y-M: Design and synthesis of tetrahydroisoquinoline derivatives as potential multidrug resistance reversal agents in cancer. Bioorg Med Chem Lett *18*: 3652-3655, 2008.

13 Hu M-K, Liao Y-F, Chen J-F, Wang B-J, Tung Y-T, Lin H-C and Lee K-P: New 1,2,3,4-tetrahydroisoquinoline derivatives as modulators of proteolytic cleavage of amyloid precursor proteins. Bioorg Med Chem *16*: 1957-1965, 2008.

14 Choquette D, Teffera Y, Polverino A and Harmange J-C: Discovery of novel 1,2,3,4-tetrahydroisoquinolines and 3,4-dihydroisoquinoline-1(2*H*)-ones as potent and selective inhibitors of KDR: synthesis, SAR, and pharmacokinetic properties. Bioorg Med Chem Lett *18*: 4054-4058, 2008.

15 Azukizawa S, Kasai M, Takahashi K, Mike T, Kunishiro K, Kanda M, Mukai C and Shirahase H: Synthesis and biological evaluation of (S)-1,2,3,4-tetrahydroisoquinoline-3-carboxylic acids: a novel series of PPARγ agonists. Chem Pharm Bull *56*: 335-345, 2008.

16 Scott JD and Williams RM: Chemistry and biology of the tetrahydroisoquinoline antitumor antibiotics. Chem Rev *102*: 1669-1730, 2002.

17 Kang JH: Salsolinol, a tetrahydroisoquinoline catechol neurotoxin, induces human Cu,Zn-superoxide dismutase modification. J Biochem Mol Biol *40*: 684-689, 2007.

18 Saitoh T, Abe K, Ishikawa M, Nakatani M, Shimazu S, Satoh N, Yoneda F, Taguchi K and Horiguchi Y: Synthesis and *in vitro* cytotoxicity of 1,2,3,4-tetrahydroisoquinoline derivatives. Eur J Med Chem *41*: 241-253, 2006.

19 Hatano H, Takekawa H, Hashimoto K, Ishihara M, Kawase M, Chu Q, Wang QT and Sakagami H: Tumor-specific cytotoxic activity of 1,2,3,4-tetrahydroisoquinoline derivatives against human oral squamous cell carcinoma cell lines Anticancer Res *29*: 3079-3086, 2009.

20 Ishihara M, Hatano H, Kawase M and Sakagami H: Estimation of relationship between the structure of 1,2,3,4-tetrahydroisoquinolin derivatives determined by a semi-empirical molecular-orbital method and their cytotoxicity. Anticancer Res *29*: 2265-2272, 2009.

21 Ishihara M, Hatano H, Takekawa F, Kawase M and Sakagami H: Estimation of relationship between descriptors and cytotoxicity of newly synthesized 1,2,3,4-tetrahydroisoquinoline derivatives. Anticancer Res 29: 4077-4082, 2009.

Received August 25, 2011
Revised October 25, 2011
Accepted October 27, 2011